The Pacific Quasi-Decadal Oscillation (QDO) – An important precursor towards anticipating major flood events in the Missouri River Basin?

Shih-Yu Wang[12*], Kirsti Hakala[2], Robert R. Gillies[12], and William J. Capehart[3]

1. Utah Climate Center, Utah State University, Logan, UT.
2. Department of Plants, Soils, and Climate, Utah State University, Logan, UT.
3. Department of Atmospheric and Environmental Sciences, South Dakota School of Mines and Technology, Rapid City, SD.

December 2013

Abstract

Measurements taken by the Gravity Recovery And Climate Experiment (GRACE) satellites indicated a continued water storage increase over the Missouri River Basin (MRB) prior to the 2011 flood event. An analysis of the major hydrologic variables in the MRB, i.e. those of soil moisture, streamflow, groundwater storage and precipitation, show a marked variability at the 10-15 year timescale coincident with the water storage increase. A climate diagnostic analysis was conducted to determine what climate forcing conditions preceded the long-term changes in these variables. It was found that precipitation over the MRB undergoes a profound modulation during the transition points of the Pacific Quasi-Decadal Oscillation (QDO) and associated teleconnections. The results infer a prominent teleconnection forcing in driving the wet/dry spells in the MRB, and this connection implies the potential for climate prediction of future wet/dry extreme events.

[*] Corresponding author: simon.wang@usu.edu, 4820 Old Main Hill, Logan, UT 84322

1. Introduction

The 2011 Midwest floods enveloped much of the Missouri and Souris River basins, causing over $2 billion dollars of damages. Thousands of acres of farmland were submerged displacing roughly 11,000 people. The human toll of the floods also included 5 fatalities. According to the U.S. Army Corps of Engineers, during May and June 2011 eastern Montana, the western Dakotas, and northern Wyoming experienced particularly heavy rainfall totals. Moreover, in the back-to-back months prior to the flooding, there was receipt of almost a year's annual runoff in the Missouri River Basin (MRB). Adding to this problem were cooler temperatures throughout the basin, which slowed the melting of the already record-high snowpack levels; this meant that much of the snowpack moisture overlapped with the precipitation and so, did not allow for either to flow out of the system prior to the inflows of the other. Although prior circumstances as early as February 2011 implied a high probability of such a spring flood, the magnitude of the flood potential was less certain. According to the National Weather Service (NWS) Assessment (2012), the scale of the event was not fully grasped until heavy rainstorms were realized over and upstream of the MRB.

In hindsight, the water storage anomaly in the MRB measured by the Gravity Recovery And Climate Experiment (GRACE) twin satellites indicated a persistent buildup of liquid water equivalent (LWE) that started as early as 2009 and peaked in the 2010-11 winter (*ref.,* Figure 1). The LWE evolution indicates a protracted accumulation of water storage as a precursor to the 2011 floods. Moreover, the geographical distribution of LWE's linear trends from 2003 to 2012 (Figure 1 inset) indicated increasing water storage over the entire MRB.

Given the aforementioned discoveries, we analyzed the major sub-components of LWE, i.e. soil moisture, streamflow and groundwater storage, in order to identify their roles in the MRB flooding event. A diagnostic analysis was then conducted to determine what climate forcing conditions preceded the long-term changes in LWE. Such climate forcing conditions were found to be oscillatory in nature and potentially predicable, suggesting that flood mitigation techniques could be implemented in the years prior to the extreme precipitation event and the floods that occurred in the MRB as a result.

2. Data

GRACE observes monthly changes in gravity caused by mass changes of the water layer, whose thickness changes (e.g., Wahr et al. 1998). The vertical extent of this water thickness is measured in centimeters; the horizontal resolution is 2° long. x 2° lat. We utilized the monthly GRACE level-3 LWE, equivalent to the total thickness of water (http://grace.jpl.nasa.gov/data/). Soil moisture data was taken from the North American Land Data Assimilation (NLDAS), which consists of uncoupled models forced with observations. Soil moisture output is measured and assimilated from 0-200cm in depth and monthly data was used from 1979 to 2011. Streamflow data were obtained from the United States Geological Survey (USGS) stream gage in Sioux City, Iowa for daily discharge (ft^3/s) from 1928 to 2013 (http://waterdata.usgs.gov/). Upstream of the Sioux City gauge, nearly 89% of the basin is regulated by the six U.S. Army Corps of Engineers reservoirs within the MRB. Groundwater well data were gathered from the Active Groundwater Level Network (http://groundwaterwatch.usgs.gov/default.asp) operated by the USGS beginning in the 1960s. We analyzed 114 active wells in South Dakota (locations are indicated in Figure 1 inset map); springtime groundwater levels were standardized prior to averaging among the 114 wells. Precipitation data were derived from the station-based, monthly Global Precipitation Climatology Centre (GPCC) dataset (Schneider et al. 2013). Atmospheric variables such as wind fields were derived from the NCEP/NCAR Global Reanalysis (Kalnay et al. 1996) starting in 1948. Sea surface temperature (SST) anomalies were obtained from the Kaplan Extended SST v2 data (Kaplan et al. 1998).

3. Results

a. Hydrologic Processes

As is shown in Figure 2a, soil moisture and streamflow in the MRB reveal marked oscillations alternating at a quasi-decadal frequency. Soil moisture and streamflow both show a prominent peak in the late 90's and a steep drop-off heading into the early 2000's. A disparity between the two becomes noticeable around 2002, where soil moisture shows a steady increase and streamflow shows a persistent decline until around 2009. Figure 2b shows the tendency of the groundwater level (i.e. current year minus the previous year) for the depiction of recharge and discharge; this also indicates a robust variability at the decadal timescale, and corresponds more strongly with soil moisture than streamflow.

The hydrologic forcing was depicted by the monthly precipitation (*ref.*, Figure 2c) averaged within the MRB boundary (Figure 1 inset) and smoothed by an 18-month running mean (to dampen the seasonal cycle). Fluctuations in the groundwater level tendency are in good agreement with the precipitation, and both time series reveal a significant quasi-decadal variability within the 10-15 year spectral power (not shown). The quasi-decadal variability in the precipitation, reflected by the alternating dry and wet spells, is particularly pronounced after the 1960s. Furthermore, the precipitation oscillation also corresponds well with the soil moisture variation at the decadal timescale.

b. Climate Forcing

The unique timescale of 10-15 years revealed from the hydrologic variables echoes an emerging climate mode – the Pacific Quasi-Decadal Oscillation (QDO) – described in a growing number of articles focusing on low-frequency variability in the Pacific SST (e.g., Allan 2000; Tourre et al. 2001; White and Tourre 2003; White and Liu 2008; Wang et al. 2011). The Pacific QDO alternates between its warm/cool status in the central equatorial Pacific near the Niño-4 region (160°E-150°W, 5°S-5°N). The Pacific QDO features a complete lifecycle with distinctive phases in terms of SST and atmospheric circulation patterns; these include the transition phases in-between the extreme warm and cold (Wang et al. 2011, 2012). We used the SST anomalies averaged in the Niño-4 region during the July-to-June annual time period to represent the Pacific QDO, hereafter referred to as "Niño-4".

The transition phases of the Pacific QDO can be depicted by the rate of change (or tendency) of Niño-4; the tendency was smoothed by a 1-2-1 moving average and is plotted in Figure 2d. Here the Niño-4 tendency was reversed in sign (explained next) and it coincides strongly with the decadal wet/dry spells of the MRB precipitation, soil moisture, streamflow and groundwater level change (Figure 2a-c). That is, the wet/dry spells experienced throughout the MRB correspond closely with the warm-to-cool/cool-to-warm transition of the Pacific QDO.

To assess the extent to which Niño-4 and the MRB precipitation are related, we computed the cross wavelet transform and wavelet coherence using monthly raw data (i.e. without any filtering or smoothing). The wavelet coherence reveals areas of high common spectral power (Torrence and Webster 1999; Grinsted et al. 2004), portrays localized correlation coefficients in time frequency and uncovers locally phase-locked behavior (Grinsted et al. 2004). As shown in Figure 2e, the wavelet spectral coherence indicates two features: (a) a concentrated significant spectrum that lies within 8-16 years that is centered at 12 years, reflecting the QDO and, (b) within the QDO frequency the phases are coherent at 90° after 1960 and at ~70° prior to 1940; this result suggests a shared spectral power peaking at 12 years with the maximum (warmest) Niño-4 leading the peak MRB precipitation by a quarter-phase (~3 years). Therefore, the statistical analysis is symptomatic of the teleconnection induced during the transition point of the Pacific QDO from one extreme phase to the other.

c. Teleconnection Processes

To depict the Pacific QDO's teleconnection pattern, the annual-mean 850-hPa streamfunction (which represents the trajectories of non-divergent low-level flow) and SST anomalies were regressed upon Niño-4 for the period of 1948-2012. All variables were subjected to a 1-2-1 (year) smoothing prior to the regression, so as to better depict decadal variability (note: the degree of freedom for significance test was thus reduced according to Bretherton et al. 1999). Linear regression function (X = a + bY) was applied respectively for SST and streamfunction as X, and for standardized Niño-4 as Y. The annual mean here covered July from the pervious year to June and Niño-4 was standardized.

The resultant regression map (Figure 3a) shows the SST pattern during the warm-phase Pacific QDO, which is El Niño-like with widespread warming in the central tropical Pacific. The SST pattern also resembles the Central Pacific (CP) type of El Niño (Ashok et al. 2007; Kao and Yu 2009) that features distinct decadal variability (Yu and Kim 2010; Furtado et al. 2011). The circulation corresponding to the warm-phase QDO reveals a predominant "zonal wave-1" pattern with cyclonic circulations prevailing in the North Pacific. However, the MRB is unaffected by any prominent circulation anomalies. Next, Figure 3b illustrates the 850-hPa circulation and SST anomalies regressed upon the Niño-4 tendency with the sign reversed (i.e. transition of the Pacific QDO). A very different teleconnection structure emerges: The relatively weak, yet statistically significant SST warming in the tropical Western Pacific excites a trans-Pacific short-wave train linking to the northwestern U.S. Such a configuration results in an increase in westerly winds towards the upper MRB. Wang et al. (2011, 2012) have shown that this short-wave train is maintained both dynamically and thermodynamically, and can be excited by tropospheric heating associated with relatively weak SST anomalies in the Western Pacific. Such a transition-phase teleconnection is embedded in the Pacific QDO's lifecycle, occurring in-between the warm and cool phases. This explains why it is the tendency of the Niño-4 (sign-reversed), rather than the Niño-4 itself, that highly correlates with the MRB precipitation.

For further examination, the circulation and SST anomalies were regressed upon the MRB precipitation. As shown in Figure 3c, a trans-Pacific wave train and the cyclonic cell over the upstream MRB appear once more. The SST warming in the western North Pacific is also visible. However, a broad region of positive SST anomalies, not depicted in Figure 3b, appears in the eastern Pacific slightly to the south of the equator; this reflects the existing, yet weak, connection of the El Niño-Southern Oscillation (ENSO) with the MRB (Mehta et al. 2011, 2012). Mo (2010) has found that the Eastern Pacific (EP)-type ENSO events induce a broader circulation anomalies over the U.S. than those produced by the CP-type ENSO, and this expands the precipitation anomalies further north into the MRB. Therefore, the EP SST signals shown in Figure 3c support the ENSO influence on the MRB at interannual timescales.

Finally, we examined any additional climate forcing that potentially made a contribution to the magnitude of the 2011 flood event. One such forcing is the North Atlantic Oscillation (NAO), which affects the U.S. through three routes: (1) a zonal circulation seesaw of the Icelandic Low (Hurrell 2003), (2) a teleconnection induced by the NAO's tropical Atlantic SST anomalies (Kushnir et al. 2010), and (3) a circumglobal teleconnection confined along the jet stream (Branstator 2002) that could impact North America from the Pacific side (Wang et al. 2010b; Schubert et al. 2012). As is revealed by the streamfunction and precipitation regressions with the NAO (Figure 3d; sign-reversed), a cyclonic circulation develops over western Canada featuring a dimension and location similar to those associated with the MRB precipitation. The cyclonic circulation leads precipitation to increase associated with westerly flows over part of the western U.S. and upper MRB. Meanwhile, a short-wave train develops over the North Pacific along the jet stream (green dotted area) and this echoes the NAO-induced circumglobal teleconnection (Branstator 2002). An extreme negative phase of the NAO occurred in 2010 and prevailed through 2011 (Figure 3d inset; sign reversed); this contributed to increased cold-season precipitation in the northern plains (Maidens et al. 2013). Moreover, the NAO has tended toward more negative phases since the late 1980s, likely in response to Atlantic multi-decadal variability (Gulev et al., 2013). Such a long-term trend also suggests a contribution of the NAO on the recent increase in the MRB precipitation and streamflow.

4. Summary and Discussion

In the MRB, interannual variability of ENSO explains less than 20% of the precipitation variation while decadal-scale variability explains over 40% (Lins and Slack 1999; Cayan et al. 1998). The quasi-decadal wet/dry spells in the MRB have long been observed (Cleaveland and Duvick 1992; Gray et al. 2004; McCabe et al. 2004; Massei et al. 2011) and are likewise in the forefront of stakeholders in the industrial and agricultural sectors tasked with the provision of energy and water (Mehta et al. 2012). When abnormal volumes of precipitation persist for longer than usual periods, such as the few years leading up to the 2011 flood, marked increases in water storage and/or flood events of severe magnitude become highly probable. Such processes have been depicted by GRACE data across the world (Reager and Famiglietti 2009). In the MRB, GRACE LWE signals seem to be dominated by soil moisture rather than groundwater level, particularly during short-lived flooding events (*ref.,* Figures 1 and 2). In fact, flooding is more likely to reflect runoff generation due to increased soil moisture rather than groundwater baseflow. In this capacity, GRACE data that summarize both soil moisture and groundwater provide a useful tool to assess and monitor the effective storage capacity in anticipation of major flood events.

There is a greater need today for decadal predictions of hydrometeorology in the MRB (Mehta et al. 2012). The fact that the MRB precipitation anomalies trail behind the warm/cool extremes of the Pacific QDO for a few years, as is identified in this study, means that such a circumstance has potential for prediction of the regional wet/dry cycles. For instance, by applying a similar lead-lag relationship between the Pacific QDO and lake level fluctuations of the Great Salt Lake (GSL) in Utah, Gillies et al. (2011) developed a prediction model for the GSL level. By capturing the shared quasi-decadal signals in Niño-4 and precipitation, the model of Gillies et al. (2011) was able to predict the lake level out to 8 years and more importantly, the timing of the GSL turnarounds. In this context, developing a similar model in the MRB seems feasible and, if successful, would prove invaluable to provide more timely and effective decision for farmers to take action in the face of impending extreme wet/dry events (e.g., by managing crops and irrigation practices). Additional research to develop such a model could help ameliorate the human and economic shock of extreme wet/dry events. Finally, as can be seen in Figure 2, precipitation and the QDO have reached the peak of its wet cycle and been heading into a dry cycle, suggestive of prolonged dry conditions for the next few years.

Acknowledgements

We would like to thank Mike Gillespie and Mark Fuchs of NWS for their assistance with streamflow data, and Kingtse Mo of CPC for soil moisture data. This research was supported by NASA grant NNX13AC37G, BOR WaterSMART grant R13AC80039, and the Utah Agricultural Experiment Station, Utah State University as journal paper number 8627.

References

Allan, R., 2000: ENSO and climatic variability in the last 150 years. *El Niño and the Southern Oscillation: Multiscale Variability, Global and Regional Impacts*, H. F. Diaz, and V. Markgrav, Eds., Cambridge Univ. Press, 3–56.

Ashok, K., S. K. Behera, S. A. Rao, H. Weng, and T. Yamagata, 2007: El Nino Modoki and its possible teleconnection. *Journal of Geophysical Research*, **112**, C11007.

Branstator, G., 2002: Circumglobal Teleconnections, the Jet Stream Waveguide, and the North Atlantic Oscillation. *J. Climate*, **15,** 1893-1910.

Bretherton, C. S., M. Widmann, V. P. Dymnikov, J. M.Wallace, and I. Blade, 1999: The effective number of spatial degrees of freedom of a time-varying field, *J. Clim.*, **12**, 1990-2009.

Cayan, D. R., M. D. Dettinger, H. F. Diaz, and N. E. Graham, 1998: Decadal Variability of Precipitation over Western North America. *J. Climate*, **11,** 3148-3166.

Cleaveland, M., and D. Duvick, 1992: Iowa climate reconstructed from tree rings, 1640-1982. *Water Resources Research*, **28,** 2607-2615.

Eicker, A., M. Schumacher, J. Kusche, H. Muller-Schmied, and P. Doll, 2013: Calibration/data assimilation approach for integrating GRACE data into the WaterGAP Global Hydrology Model using an ensemble Kalman filter. *Using GRACE Data for Water Cycle Analysis and Climate Modeling*.

Furtado, J. C., E. Di Lorenzo, N. Schneider, and N. A. Bond, 2011: North Pacific decadal variability and climate change in the IPCC AR4 models. *J. Climate*, **24,** 3049-3067.

Gillies, R. R., O.-Y. Chung, S.-Y. Wang, and P. Kokoszka, 2011: Incorporation of Pacific SSTs in a time series model towards a longer-term forecast for the Great Salt Lake elevation. *J. Hydrometeor.*, **12,** 474-480.

Gray, S. T., C. L. Fastie, S. T. Jackson, and J. L. Betancourt, 2004: Tree-ring-based reconstruction of precipitation in the Bighorn Basin, Wyoming, since 1260 AD. *J. Climate*, **17,** 3855-3865.

Grinsted, A., J. C. Moore, and S. Jevrejeva, 2004: Application of the cross wavelet transform and wavelet coherence to geophysical time series. *Nonlinear processes in geophysics*, **11,** 561-566.

Gulev, S. K., M. Latif, N. Keenlyside, W. Park, and K. P. Koltemann, 2013: North Atlantic Ocean control on surface heat flux on multidecadal timescales. *Nature*, **499**, 464-467.

Hurrell, J. W., 2003: *The North Atlantic oscillation: climatic significance and environmental impact.* Vol. 134, American Geophysical Union, 279 pp.

Kalnay, E., and Coauthors, 1996: The NCEP/NCAR 40-Year Reanalysis Project. *Bull. Amer. Meteor. Soc.*, **77,** 437-471.

Kao, H.-Y., and J.-Y. Yu, 2009: Contrasting eastern-Pacific and central-Pacific types of ENSO. *J. Climate*, **22,** 615-632.

Kaplan, A., M. Cane, Y. Kushnir, A. Clement, and coauthors, 1998: Analyses of global sea surface temperature 1856-1991. *J. Geophys. Res.*, **103,** 18567-18589.

Konikow, L. F., 2013: *Groundwater Depletion in the United States (1900-2008).* US Department of the Interior, US Geological Survey.

Kushnir, Y., R. Seager, M. Ting, N. Naik, and J. Nakamura, 2010: Mechanisms of Tropical Atlantic SST Influence on North American Precipitation Variability. *J. Climate*, **23,** 5610-5628.

Lins, H. F., and J. R. Slack, 1999: Streamflow trends in the United States. *Geophy. Res. Lett.*, **26,** 227-230.

Maidens, A., A. Arribas, A. A. Scaife, C. MacLachlan, D. Peterson, and J. Knight, 2013: The Influence of Surface Forcings on Prediction of the North Atlantic Oscillation Regime of Winter 2010-11. *Mon. Wea. Rev.*

Massei, N., B. Laignel, E. Rosero, A. Motelay-massei, J. Deloffre, Z. Yang, and A. Rossi, 2011: A wavelet approach to the short-term to pluri-decennal variability of streamflow in the Mississippi river basin from 1934 to 1998. *Inter. J. Climatol.*, **31,** 31-43.

McCabe, G. J., M. A. Palecki, and J. L. Betancourt, 2004: Pacific and Atlantic Ocean influences on multidecadal drought frequency in the United States. *Proc. Natl. Acad. Sci.*, **101,** 4136-4141.

Mehta, V. M., and coauthors, 2012: Decadal Climate Information Needs of Stakeholders for Decision Support in Water and Agriculture Production Sectors: A Case Study in the Missouri River Basin. *Weather, Climate, and Society*, **5,** 27-42.

Mo, K. C., 2010: Interdecadal Modulation of the Impact of ENSO on Precipitation and Temperature over the United States. *J. Climate*, **23,** 3639-3656.

NWS-Assessment, 2012: The Missouri/Souris River Floods of May-August 2011. U. S. Dpeartment of Commerce, NOAA, National Weather Service, http://www.nws.noaa.gov/os/assessments/pdfs/Missouri_floods11.pdf.

Reager, J. T., and J. S. Famiglietti, 2009: Global terrestrial water storage capacity and flood potential using GRACE. *Geophy. Res. Lett.*, **36,** L23402.

Schneider, U., A. Becker, P. Finger, A. Meyer-Christoffer, M. Ziese, and B. Rudolf, 2013: GPCC's new land surface precipitation climatology based on quality-controlled in situ data and its role in quantifying the global water cycle. *Theoretical and Applied Climatology*, **115**, 1-26.

Torrence, C., and P. J. Webster, 1999: Interdecadal changes in the ENSO-monsoon system. *J. Climate*, **12,** 2679-2690.

Tourre, Y., B. Rajagopalan, Y. Kushnir, M. Barlow, and W. White, 2001: Patterns of Coherent Decadal and Interdecadal Climate Signals in the Pacific Basin During the 20 th Century. *Geophys. Res. Lett.*, **28,** 2069-2072.

Wahr, J., M. Molenaar, and F. Bryan, 1998: Time variability of the Earth's gravity field: Hydrological and oceanic effects and their possible detection using GRACE. *Journal of Geophysical Research: Solid Earth*, **103,** 30205-30229.

Wang, S.-Y., R. R. Gillies, and T. Reichler, 2012: Multi-decadal drought cycles in the Great Basin recorded by the Great Salt Lake: Modulation from a transition-phase teleconnection. *J. Climate*, **25,** 1711-1721.

Wang, S.-Y., R. R. Gillies, J. Jin, and L. E. Hipps, 2010a: Coherence between the Great Salt Lake Level and the Pacific Quasi-Decadal Oscillation. *J. Climate*, **23,** 2161-2177.

Wang, S.-Y., R. R. Gillies, L. E. Hipps, and J. Jin, 2011: A transition-phase teleconnection of the Pacific quasi-decadal oscillation. *Clim. Dynamics*, **36,** 681-693.

Wang, S.-Y., L. E. Hipps, R. R. Gillies, X. Jiang, and A. L. Moller, 2010b: Circumglobal teleconnection and early summer rainfall in the US Intermountain West. *Theor. Appl. Climatol.*, **102,** 245-252.

White, W. B., and Y. M. Tourre, 2003: Global SST/SLP waves during the 20th century. *Geophys. Res. Lett.*, **30,** 53-51 - 53-54.

White, W. B., and Z. Liu, 2008: Resonant excitation of the quasi-decadal oscillation by the 11-year signal in the Sun's irradiance. *J. Geophys. Res.*, **113,** 1-16.

Yu, J.-Y., and S. T. Kim, 2010: Relationships between Extratropical Sea Level Pressure Variations and the Central Pacific and Eastern Pacific Types of ENSO. *J. Climate*, **24,** 708-720.

Figure Captions

Figure 1. Monthly anomalies of liquid water equivalent (LWE; cm) derived from GRACE averaged within the Missouri River Basin; domain is outlined in the inset map. Blue/yellow areas indicate positive/negative LWE anomalies from the long-term mean. Inset: Geographical distribution of the linear trend in LWE over the period of January 2003-December 2012, with blue/red areas indicating decreasing/increasing LWE. The white dots in South Dakota indicate the 114 groundwater wells analyzed.

Figure 2. (a) Annual streamflow in Sioux City, Iowa (black) overlaid with soil moisture over the MRB at top 200cm (green), both time series are standardized. (b) Tendency (time derivative) of spring groundwater level from 114 wells in South Dakota. (c) Monthly precipitation anomalies averaged within the MRB smoothed by a 1-2-1 running mean (in mm/day; blue is positive and orange is negative). (d) Tendency of the NINO4 index representing the Pacific QDO transitions. (e) Wavelet spectral coherence (shading) and phase difference (vectors) between the monthly precipitation and NINO4 – only the significant spectra (95%; outlined by white contours) are overlaid with phase vectors. A 90° (270°) phase difference means that NINO4 leads (lags) precipitation by a quarter-phase, i.e. 3 years at the 12-year frequency.

Figure 3. Annual-mean 850-hPa streamfunction (contours) and SST anomalies (shadings) regressed respectively upon (a) NINO4, (b) NINO4 tendency, (c) MRB precipitation, and (d) sign-reversed NAO. Shadings reflect values significant above the 90% level per *t*-test. In (d) the shadings are the precipitation regression and the green dotted area denotes the jet stream with 200-hPa wind speed greater than 20 m/s. The inset in (d) is

the annual NAO index and its 20-year lowpassed trend, sign reversed. The blue arrow lines indicate the trans-Pacific short-wave train. The MRB is outlined in (c) and (d).

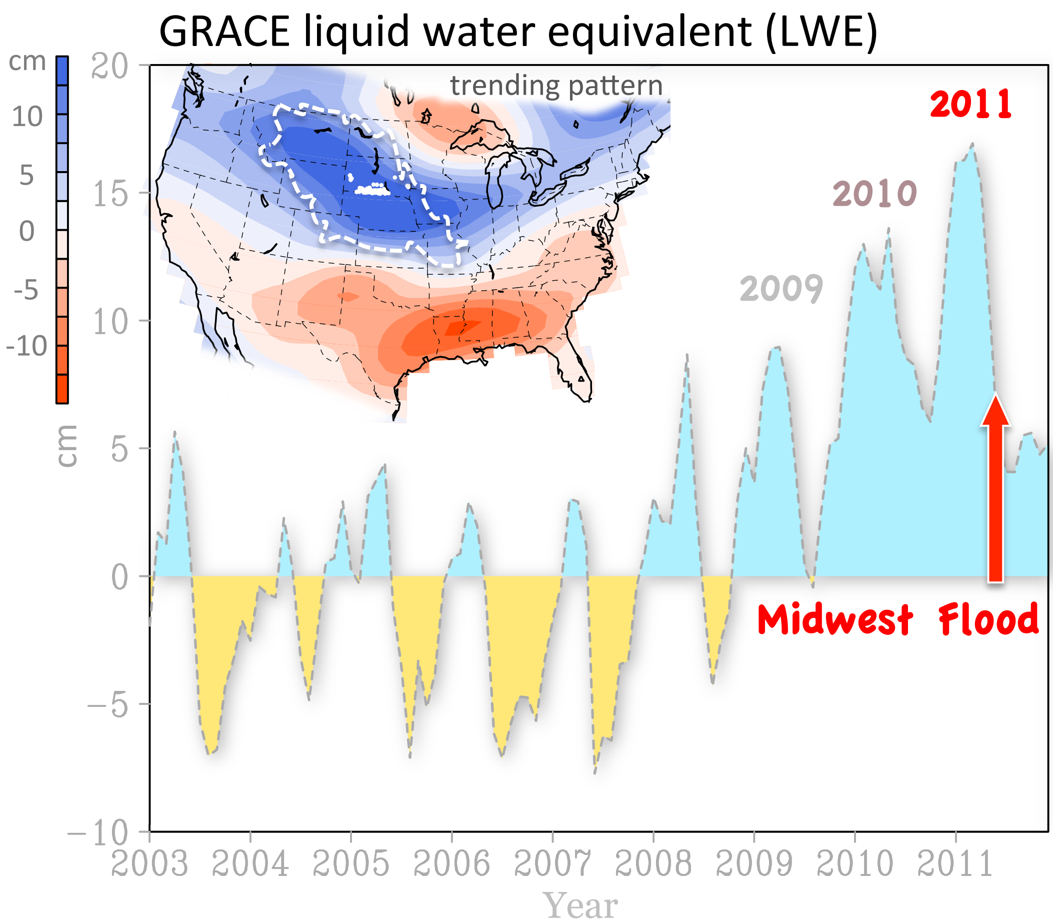

Figure 1. Monthly anomalies of liquid water equivalent (LWE; cm) derived from GRACE averaged within the Missouri River Basin; domain is outlined in the inset map. Blue/yellow areas indicate positive/negative LWE anomalies from the long-term mean. Inset: Geographical distribution of the linear trend in LWE over the period of January 2003-December 2012, with blue/red areas indicating decreasing/increasing LWE. The white dots in South Dakota indicate the 114 groundwater wells analyzed.

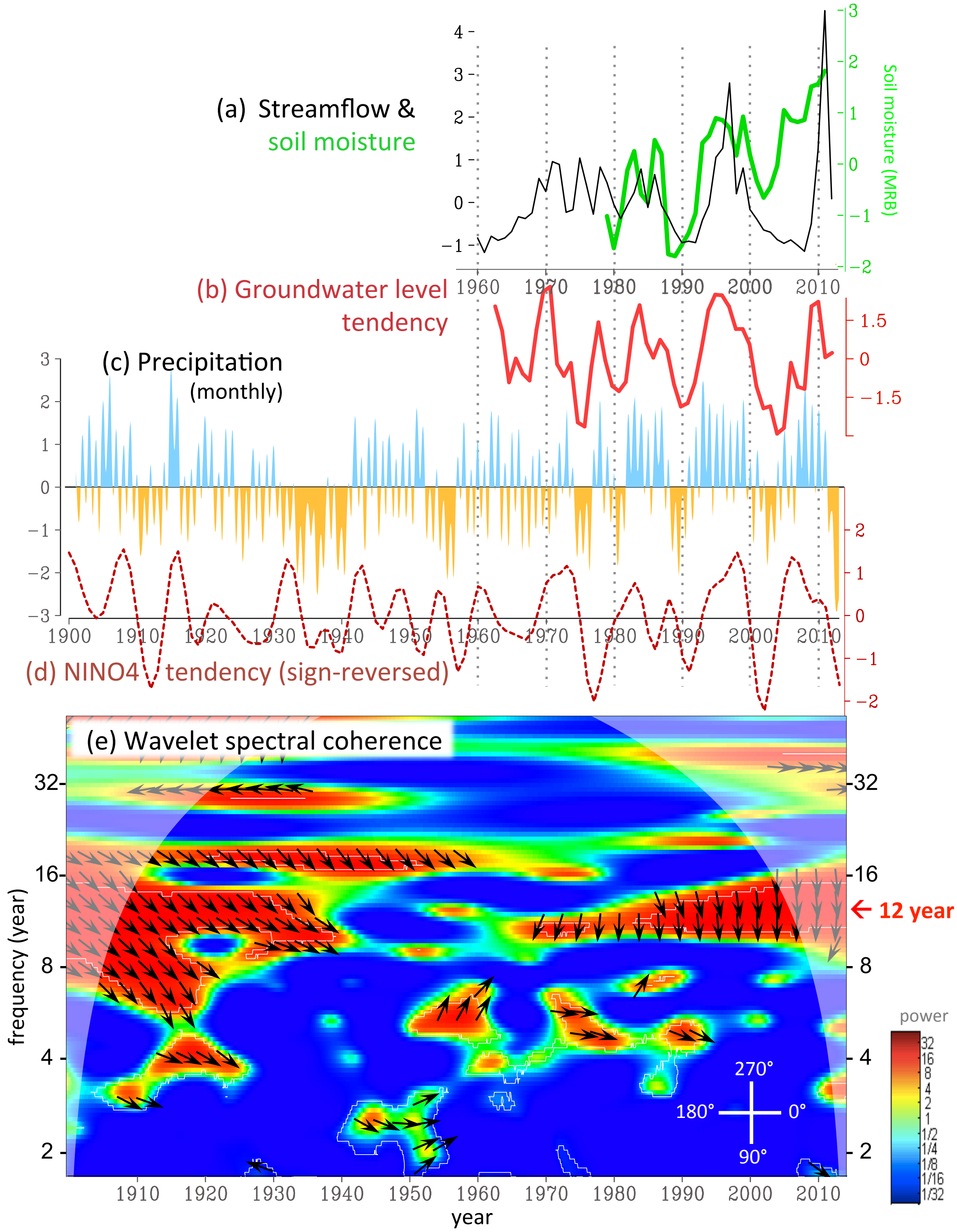

Figure 2. (a) Annual streamflow in Sioux City, Iowa (black) overlaid with soil moisture over the MRB at top 200cm (green), both time series are standardized. (b) Tendency (time derivative) of spring groundwater level from 114 wells in South Dakota. (c) Monthly precipitation anomalies averaged within the MRB smoothed by a 1-2-1 running mean (in mm/day; blue is positive and orange is negative). (d) Tendency of the NINO4 index representing the Pacific QDO transitions. (e) Wavelet spectral coherence (shading) and phase difference (vectors) between the monthly precipitation and NINO4 – only the significant spectra (95%; outlined by white contours) are overlaid with phase vectors. A 90° (270°) phase difference means that NINO4 leads (lags) precipitation by a quarter-phase, i.e. 3 years at the 12-year frequency.

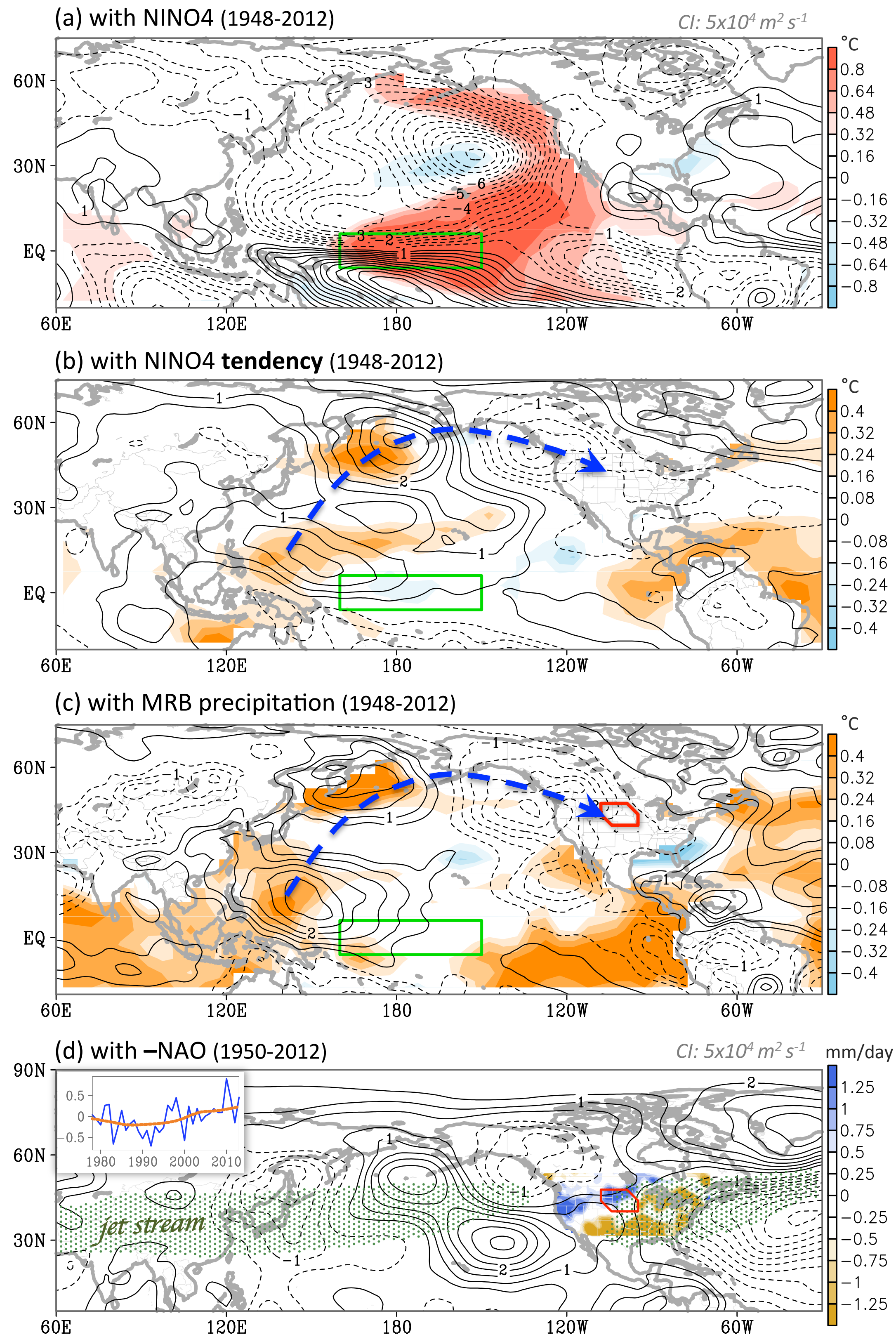

Figure 3. Annual-mean 850-hPa streamfunction (contours) and SST anomalies (shadings) regressed respectively upon (a) NINO4, (b) NINO4 tendency, (c) MRB precipitation, and (d) sign-reversed NAO. Shadings reflect values significant above the 90% level per *t*-test. In (d) the shadings are precipitation regression and the green dotted area denotes the jet stream with 200-hPa wind speed greater than 20 m/s. The inset in (d) is the annual NAO index and its 20-year lowpassed trend, sign reversed. The blue arrow lines indicate the trans-Pacific short-wave train. The MRB is outlined in (c) and (d).